Fundamental Frequencies of Satellite Relative Motion and Control of Formations

Srinivas R. Vadali,* Prasenjit Sengupta,† Hui Yan,‡ and Kyle T. Alfriend§
Texas A&M University, College Station, Texas 77843-3141

Expressions for the fundamental natural frequencies associated with J_2-perturbed relative motion of satellites in near-circular orbits are derived. Special values of the orbit inclination, dependent on initial conditions, are obtained, for which the in-plane and out-of-plane fundamental frequencies remain equal to each other over an extended period of time, resulting in nonprecessing relative orbits. This result validates and generalizes a similar finding, based on numerical investigations by other researchers. The analysis is extended to the developments of accurate prediction and control models for fuel-optimal formation maintenance and intersatellite fuel balancing. Numerical simulation results are presented to demonstrate the accuracy of the developed models and the effects of frequency matching on control requirements.

Nomenclature

a	=	semimajor axis
e	=	eccentricity
i	=	inclination
J	=	performance index
J_2	=	second zonal harmonic coefficient of the Earth's gravity field
M	=	mean anomaly
n_0	=	two-body mean motion of the chief
n_{xy}	=	in-plane fundamental frequency of the deputy
n_z	=	cross-track fundamental frequency of the deputy
$\mathfrak{o}$	=	osculating orbital element vector
$\bar{\mathfrak{o}}$	=	mean orbital element vector
R	=	radial distance of satellite from Earth
R_e	=	equatorial radius of Earth
t	=	time
u	=	acceleration
$\mathbf{x}$	=	relative position vector
$\dot{\mathbf{x}}$	=	relative velocity vector
$\mathbf{x}_r$	=	reference relative position vector
$\dot{\mathbf{x}}_r$	=	reference relative velocity vector
(x, y, z)	=	relative position coordinates (radial, along-track, out-of-plane)
α	=	formation phase angle
Δ	=	differential
ρ	=	radius of the projected circular relative orbit
ρ_x	=	amplitude of the radial component of relative motion
ρ_z	=	amplitude of the cross-track component of relative motion
(ϕ, ψ)	=	in-plane and cross-track phase angles
Ω	=	longitude of the ascending node
ω	=	argument of perigee

Subscripts

0	=	referenced to chief
1	=	referenced to deputy

Received 25 September 2007; accepted for publication 5 February 2008.

*Stewart & Stevenson-I Professor, Department of Aerospace Engineering, MS 3141; svadali@aero.tamu.edu. Associate Fellow AIAA.

†Research Associate, Department of Aerospace Engineering, MS 3141; prasenjit@tamu.edu. Member AIAA.

‡Research Associate, Department of Aerospace Engineering, MS 3141; h0y8618@aeromail.tamu.edu. Member AIAA.

§Texas Engineering Experiment Station Distinguished Research Chair Professor, Department of Aerospace Engineering, MS 3141; alfriend@aero.tamu.edu. Fellow AIAA.

Introduction

SATELLITE formation flying has been an active area of research over the last decade and continues to attract much attention. Several missions are being planned to achieve a variety of objectives, such as the deployment of distributed spacecraft systems and imaging extra-solar planets [1]. Low thrust requirements for formation flight applications have also led to the developments of novel electric thrusters and the use of electromagnetic [2] and electrostatic forces [3].

Preliminary design of the relative orbits for formation flight is based typically on the Hill–Clohessy–Wiltshire (HCW) equations [4], valid for circular reference orbits of the two-body problem. Two, nontrivial periodic solutions to the HCW equations are the projected circular orbit (PCO) and the general circular orbit (GCO). The PCO, which appears circular when viewed along the zenith-nadir directions of the reference satellite (chief), has been found suitable for the synthesis of sparse apertures in space. A satellite (deputy) in a GCO maintains a constant separation distance, in three-dimensional space, relative to the chief. Relationships between PCO and GCO position and velocity variables, differential orbital elements, and integration constants have been presented in various forms in [5–14]. Conditions for establishing bounded relative orbits via nonlinearity and eccentricity corrections and energy matching have been provided in [15–19]. A variety of continuous and impulsive control methods for formation maintenance have also been proposed [20–26]. A methodology for accommodating the J_2 disturbance, for the dual purposes of minimizing formation-maintenance cost and balancing the intersatellite fuel budgets, has also been treated in [12,13].

Coupled, linearized differential equations with periodic coefficients [27–29] have been developed for J_2-perturbed relative motion. Although these equations allow the application of linear design methodologies for formation maintenance and control, they do not provide simple analytical solutions to the motion variables. Unlike the HCW equations, which admit periodic solutions with the same natural frequencies for all the three axes, the perturbed equations exhibit different in-plane and out-of-plane frequencies. It has been stated, without proof, in [30,31], that the in-plane fundamental frequency is the anomalistic period, i.e., perigee-to-perigee period, and that the cross-track motion is based on nodal crossing of the reference satellite. This difference in the two frequencies results in the precession of the relative orbit. Recently, Sabatini et al. [32] used a genetic algorithm-based approach to obtain

two special values of the orbit inclination, for which the perturbed relative orbits neither precess nor distort appreciably, over a period of nearly one day. A detailed explanation of the reasons behind their numerical observations is one of the contributions of the present paper.

This paper begins with a geometric description of satellite relative motion using the unit-sphere approach [33]. The expressions for the in-plane and cross-track motion variables are linearized to extract the fundamental frequencies. Formulas for determining the PCO initial conditions (valid even for nonequatorial circular orbits) are derived in terms of the classical differential orbital elements. Next, a condition on the orbit inclination for matching the in-plane and cross-track fundamental natural frequencies over a finite horizon is presented. The analysis is extended to relate the natural frequencies to the control requirements for formation maintenance and fuel balancing among the satellites in a PCO formation. The inefficiency of radial thrusting for formation maintenance in the presence of J_2 is formally brought to light via the use of a set of modified HCW equations. The implementation of a feedback control law based on a linear quadratic regulator (LQR), augmented by an averaging filter [34] to remove the short-periodic variations in the relative motion state variables, is discussed. The paper ends with the presentation of numerical simulation results validating the analytical models, followed by the conclusions.

Geometry of Relative Motion

The unit-sphere approach [33] provides analytical expressions for the relative motion variables in terms of the differential orbital elements as given here:

$$x = -R_0 + R_1 \left\{ \begin{array}{c} \cos^2(i_0/2)\cos^2(i_1/2)\cos(\Delta\theta + \Delta\Omega) \\ +\sin^2(i_0/2)\sin^2(i_1/2)\cos(\Delta\theta - \Delta\Omega) \\ +\sin^2(i_0/2)\cos^2(i_1/2)\cos(2\theta_0 + \Delta\theta + \Delta\Omega) \\ +\cos^2(i_0/2)\sin^2(i_1/2)\cos(2\theta_0 + \Delta\theta - \Delta\Omega) \\ +1/2\sin(i_0)\sin(i_1)[\cos(\Delta\theta) - \cos(2\theta_0 + \Delta\theta)] \end{array} \right\} \tag{1}$$

$$y = R_1 \left\{ \begin{array}{c} \cos^2(i_0/2)\cos^2(i_1/2)\sin(\Delta\theta + \Delta\Omega) \\ +\sin^2(i_0/2)\sin^2(i_1/2)\sin(\Delta\theta - \Delta\Omega) \\ -\sin^2(i_0/2)\cos^2(i_1/2)\sin(2\theta_0 + \Delta\theta + \Delta\Omega) \\ -\cos^2(i_0/2)\sin^2(i_1/2)\sin(2\theta_0 + \Delta\theta - \Delta\Omega) \\ +1/2\sin(i_0)\sin(i_1)[\sin(\Delta\theta) + \sin(2\theta_0 + \Delta\theta)] \end{array} \right\} \tag{2}$$

$$\begin{aligned} z = R_1\{&[\sin i_1 \cos i_0 - \cos i_1 \sin i_0 \cos\Delta\Omega]\sin\theta_1 \\ &- \sin i_0 \sin\Delta\Omega \cos\theta_1\} \end{aligned} \tag{3}$$

where x, y, and z are, respectively, the radial, in-plane, and out-of-plane separations between the two satellites. The subscripts 0 and 1, respectively, indicate references to the chief and deputy satellites. The radius of a satellite is denoted by R, $\Delta\Omega$ is the differential longitude of the ascending node, θ is the latitude angle, $\Delta\theta$ is the differential argument of latitude, and i denotes the orbit inclination. It is assumed herein that the reference orbit is nonequatorial.

Equations (1–3) are geometrically exact and valid for large differences between the respective orbital elements of the two satellites. Considering mean orbital elements, and by neglecting the effects of the secular terms in Eq. (3), it can be shown that the out-of-plane fundamental frequency is the mean motion of the deputy. The in-plane motion equations are more complicated, involving the sums and differences of several frequencies. The fundamental frequency of periodic motion in the two-body problem is the mean motion of the chief. The fundamental frequencies for perturbed relative motion are the subjects of the subsequent sections.

It can be shown from Eqs. (1–3) that the following results hold for small relative motion:

$$x \approx R_1 - R_0 \tag{4}$$

$$y \approx R_0(\Delta\theta + \Delta\Omega\cos i_0) \tag{5}$$

$$z \approx R_0(\Delta i \sin\theta_1 - \sin i_0 \Delta\Omega \cos\theta_1) \tag{6}$$

Equation (6) is not in its simplest form and can easily be reduced further by approximating the latitude angle of the deputy by that of the chief. However, as shown next, such an approximation is not necessary. Equations (4–6) can be simplified by using first-order eccentricity expansions for R and θ:

$$R \approx a(1 - e\cos M) \tag{7}$$

$$\theta \approx \omega + M + 2e\sin M \tag{8}$$

$$\sin\theta \approx \sin\lambda - e\sin\omega \tag{9}$$

$$\cos\theta \approx \cos\lambda - e\cos\omega \tag{10}$$

where a, e, ω, and M are, respectively, the semimajor axis, eccentricity, argument of perigee, and mean anomaly. Note that $\lambda = M + \omega$ is the mean argument of latitude. For orbits with small eccentricities, even for small relative motion, ΔM and $\Delta\omega$ can be large, but $\Delta\lambda$ remains small. Hence, trigonometric functions of ΔM and $\Delta\omega$ appearing in the relative motion expressions should not be approximated by linearization. As will be shown next, the use of nonsingular elements, for near-circular orbits, is not necessary for deriving the main results in this paper.

The following equations are obtained by substituting Eqs. (7–10) in Eqs. (4–6) and neglecting the higher harmonics of motion:

$$x \approx \Delta a + a_0[(e_1\sin\Delta M)\sin M_0 + (e_0 - e_1\cos\Delta M)\cos M_0] \tag{11}$$

$$\begin{aligned} y \approx\ & a_0[\Delta\lambda + \Delta\Omega\cos i_0 - e_0(e_1\sin\Delta M)] \\ &+ 2a_0[-(e_0 - e_1\cos\Delta M)\sin M_0 + (e_1\sin\Delta M)\cos M_0] \end{aligned} \tag{12}$$

$$\begin{aligned} z \approx a_0\Big[&\Delta i\sin\lambda_1 - \sin i_0\Delta\Omega\cos\lambda_1 \\ &- \frac{3}{2}e_0(\Delta i\sin\omega_1 - \sin i_0\Delta\Omega\cos\omega_1)\Big] \end{aligned} \tag{13}$$

It has been shown that unlike for two-body motion, the differential semimajor axis Δa has to be $\mathcal{O}(J_2)$ for J_2-invariant orbits [35] and, in general, for preventing along-track secular drift [29]. Equations (11–13) show the presence of bias and/or long-periodic components in all three of the relative motion directions, induced due to the effects of eccentricity and J_2.

In-Plane Natural Frequency for Formations in Near-Circular Orbits

In this paper, the eccentricity of a near-circular orbit is assumed to be consistent with the first-order eccentricity expansion, i.e., $e_0 \leq 0.001$. As can be seen from Eqs. (11) and (12), for circular orbits ($e_0 = 0$), the in-plane fundamental frequency is the mean motion of the deputy: $n_{xy} = \dot{M}_1$. For small formations ($\approx$1 km) in near-circular orbits, $e_1 \approx e_0$. Bounds on the in-plane frequency can be obtained by representing the aforementioned motion variables by their respective mean values, secular drift rates, and periodic components:

$$x \approx \Delta a + \rho_x \sin(M_0 + \phi) \tag{14}$$

$$y \approx a_0\{\Delta\lambda(0) + \Delta\Omega(0)\cos i_0 - e_0[e_1 \sin \Delta M(0)]\} + a_0[\Delta\dot{\lambda} + \Delta\dot{\Omega}\cos i_0]t + 2\rho_x \cos(M_0 + \phi) \tag{15}$$

where

$$\rho_x = a_0\sqrt{[(e_1 \sin \Delta M)^2 + (e_0 - e_1 \cos \Delta M)^2}} \tag{16}$$

$$\phi = \tan^{-1}\left[\frac{e_0 - e_1 \cos \Delta M}{e_1 \sin \Delta M}\right] \tag{17}$$

and t indicates time. The phase angle ϕ is not constant due to the differential mean anomaly rate. Equations (16) and (17) show that, for circular orbits, with the use of mean elements, ρ_x is a constant and $\phi = -\pi/2 + \Delta M$. For the case of $e_1 \approx e_0$, $\phi = \Delta M/2$.

An eccentricity-dependent expression for the in-plane frequency can easily be derived from the preceding information. However, for the preceding two extreme cases considered, it can be bounded by $\dot{M}_1$ and $0.5(\dot{M}_0 + \dot{M}_1)$. As a further simplification, it is assumed in the rest of the paper that $n_{xy} \approx \dot{M}_1 \approx \dot{M}_0$. This result is in agreement with the observations made in [30,31].

Cross-Track Fundamental Frequency

The procedure for determining the cross-track fundamental frequency is similar to that presented in the previous section. Equation (13) can be represented as follows:

$$z \approx \rho_z \sin(\lambda_1 + \psi) - \frac{3}{2}\rho_z e_0 \sin(\omega_1 + \psi) \tag{18}$$

where

$$\rho_z \approx a_0\sqrt{\Delta i^2 + [\Delta\Omega(0) + \Delta\dot{\Omega}t]^2 \sin^2 i_0} \tag{19}$$

$$\psi = \tan^{-1}\left[-\frac{[\Delta\Omega(0) + \Delta\dot{\Omega}t]\sin i_0}{\Delta i}\right] \tag{20}$$

It can be shown by differentiating Eq. (20) that

$$\dot{\psi} = \frac{-\Delta\dot{\Omega}\Delta i \sin i_0}{\Delta i^2 + (\Delta\Omega \sin i_0)^2} \tag{21}$$

As can be seen from the preceding equation, $\dot{\psi}$ is not a constant due to differential nodal precession. However, focusing attention on a small time scale and ignoring the effect of $\Delta\dot{\Omega}$ in the denominator of the preceding equation, an estimate of the rate of change of the cross-track phase angle is obtained as follows:

$$\dot{\psi} \approx \frac{-\Delta\dot{\Omega}\Delta i \sin i_0}{\Delta i^2 + [\Delta\Omega(0)\sin i_0]^2} \tag{22}$$

Hence, the cross-track natural frequency n_z can be approximated as shown next:

$$n_z \approx \dot{M}_1 + \dot{\omega}_1 - \frac{\Delta\dot{\Omega}\Delta i \sin i_0}{\Delta i^2 + [\Delta\Omega(0)\sin i_0]^2} \tag{23}$$

The result presented here is accurate to $\mathcal{O}(J_2)$ and valid for near-circular orbits, over a finite period of time ($\approx$ one day).

Initial Conditions

Procedures for determining the initial conditions for perturbed PCO and GCO have been presented in [12,13], based on the solutions to the HCW equations. The treatment herein uses the approximate solutions to the relative motion variables presented earlier for near-circular orbits. It is convenient to key in the initial conditions to the initial state of the chief satellite, but given the form of the aforementioned natural solutions, they are derived more conveniently, with respect to the deputy's mean argument of latitude.

Considering the PCO initial conditions, the assumed forms for the along-track and cross-track relative motion variables are, respectively,

$$y(0) = \rho(0)\cos[\lambda_1(0) + \alpha(0)] \tag{24}$$

$$z(0) = \rho(0)\sin[\lambda_1(0) + \alpha(0)] \tag{25}$$

where $\alpha(0)$ is the desired initial phase angle and $\rho(0)$ is the initial radius of the PCO, in the y-z plane. Note that, in contrast to the forms used for describing the natural relative motion variables, the same phase angle is used for both $x(0)$ and $y(0)$ for the purpose of establishing PCO initial conditions. Upon comparing Eqs. (15) and (18) with Eqs. (24) and (25), respectively, it is evident that $\rho_x = 0.5\rho(0)$ and $\rho_z = \rho(0)$.

It can be shown from Eqs. (12), (13), (24), and (25) that, for near-circular orbits, the differential orbital elements can be computed from the equations shown next:

$$\Delta\lambda(0) + \Delta\Omega(0)\cos i_0 = \frac{\rho(0)e_0}{2a_0}\cos[\omega_0(0) + \alpha(0)] \tag{26}$$

$$e_1 \sin \Delta M(0) = \frac{\rho(0)}{2a_0}\cos[\omega_0(0) + \alpha(0)] \tag{27}$$

$$e_1 \cos \Delta M(0) = e_0 - \frac{\rho(0)}{2a_0}\sin[\omega_0(0) + \alpha(0)] \tag{28}$$

$$\Delta\Omega(0) = -\frac{\rho(0)}{a_0 \sin i_0}\sin\alpha(0) \tag{29}$$

$$\Delta i = \frac{\rho(0)}{a_0}\cos\alpha(0) \tag{30}$$

Terms involving $[\rho(0)/a_0]^2$ have been neglected in the derivation of the preceding equations. Except for the case of equatorial reference orbits, Eqs. (26–30) do not contain singularities. It is reiterated that the analysis presented in this paper is valid for nonequatorial reference orbits. For circular orbits, $\omega_0(0)$ can be selected arbitrarily.

Notice the presence of an eccentricity-induced bias term in the right-hand side of Eq. (26), rendering the relative orbit slightly off center in the along-track direction. This result matches with the corresponding initial condition expression derived in [11], for first-order eccentricity expansions. Equations (27) and (28) can be used to calculate e_1 and $\Delta M(0)$, enabling the computation of Δe. It can be seen that for circular reference orbits, $\Delta e = \rho(0)/2a_0$ and $\tan \Delta M(0) = -\cot[\omega_0(0) + \alpha(0)]$. Hence, for circular orbits, unlike $\Delta M(0)$, Δe is independent of $\omega_0(0)$ and $\alpha(0)$. Finally, $\Delta\lambda(0)$ can be determined from Eqs. (26) and (29). The required change in the semimajor axis is obtained from the rate-matching constraint [29]:

$$\frac{\Delta a}{a_0} = -\frac{J_2}{2}\left(\frac{R_e}{a_0}\right)^2 \frac{3\eta_0 + 4}{\eta_0^4}\left[(1 - 3\cos^2 i_0)\frac{e_0\Delta e}{\eta_0^2} + \Delta i \sin 2i_0\right] \tag{31}$$

where $\eta_0 = \sqrt{(1 - e_0^2)}$.

The condition given by Eq. (31) is one of several others that can be used to minimize drift between two satellites. Numerical approaches can also be used to determine initial conditions to minimize drift in both along-track as well as cross-track directions. Breger [36] has presented a method based on convex linear optimization and Yan et al. [37] have adopted the method of differential corrections. Both of the aforementioned methods can handle more general perturbations other than J_2. The previous equations provide mean classical differential orbit element initial conditions for PCO.

Matching In-Plane and Cross-Track Fundamental Frequencies

As mentioned earlier, a mismatch between the in-plane and cross-track frequencies causes precession of the relative orbit. A condition for matching the two frequencies is derived in this section. It can be seen from Eq. (23), and the result $n_{xy} \approx \dot{M}_1$, that the difference between the in-plane and cross-track frequencies over a short time interval (compared with the period of the differential nodal precession rate) is

$$n_z - n_{xy} = \dot{\omega}_1 - \frac{\Delta\dot{\Omega}\Delta i \sin i_0}{\Delta i^2 + [\Delta\Omega(0)\sin i_0]^2} \tag{32}$$

The drift rates for the argument of perigee and nodal difference, respectively, can be written as

$$\dot{\omega}_0 = -k\left(2 - \frac{5}{2}\sin^2 i_0\right) \tag{33}$$

and

$$\Delta\dot{\Omega} = -k \sin i_0 \Delta i \tag{34}$$

where

$$k = -1.5 J_2 \left(\frac{R_e}{a_0}\right)^2 n_0 \tag{35}$$

Neglecting the effect of $\Delta\dot{\omega}$ in Eq. (32), the frequency mismatch is estimated as follows:

$$n_z - n_{xy} = k\sin^2 i_0 \left(\frac{5}{2} + \frac{\Delta i^2}{\Delta i^2 + [\Delta\Omega(0)\sin i_0]^2}\right) - 2k \tag{36}$$

For the special case of the PCO, substitution of Eqs. (29) and (30) into Eq. (36) leads to the following result:

$$i_0^* = \sin^{-1}\left(\sqrt{\frac{2}{2.5 + \cos^2\alpha(0)}}\right) \tag{37}$$

Thus, the frequency-matching condition is satisfied by two possible values of the chief's orbit inclination for any $\alpha(0)$. The inclinations for $\alpha(0) = 0$ are $i_0^* = 49.11$ and 130.89 deg, and those for $\alpha(0) = 90$ deg are the critical inclination values: $i_0^* = 63.43$ and 116.57 deg. The numerical results presented in [32] agree very closely with the special inclination values determined here.

Figure 1 shows 15 relative motion orbits for a 7100 km circular reference orbit with $\alpha(0) = 0$ and $i_0 = 49.11$ deg. Figure 2 shows the same for a polar orbit, with $\alpha(0) = 0$. The effect of the frequency-matching condition is obvious from the two figures. The mismatch in the in-plane and cross-track frequencies results in the precession of the PCO shown in Fig. 2. If allowed to continue in this manner indefinitely, without control, the PCO of Fig. 1 will also distort due to the effect of differential nodal precession.

It can be shown by substituting Eq. (34) into Eq. (22) and using Eqs. (29) and (30) that, for a PCO formation, the natural rate of change of the cross-track phase angle, for each satellite with a different initial phase angle, is given by

$$\dot{\psi} = k\sin^2 i_0 \cos^2\alpha(0) \tag{38}$$

Considering an infinite number of satellites (formation), the average rate of change of the phase angle can be obtained as shown next:

$$\dot{\psi}_{\text{av}} = \frac{1}{2} k \sin^2 i_0 \tag{39}$$

Note that, under the assumptions in this paper, $\dot{\psi}$ is not a function of the size of the relative orbit.

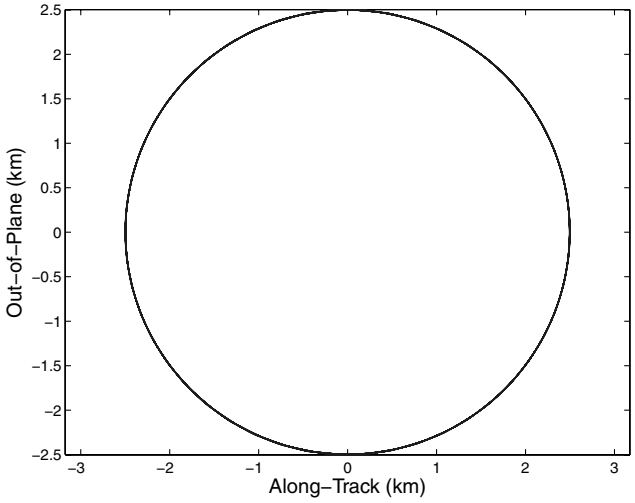

Fig. 1 Relative orbits for $i_0 = 49.11$ deg.

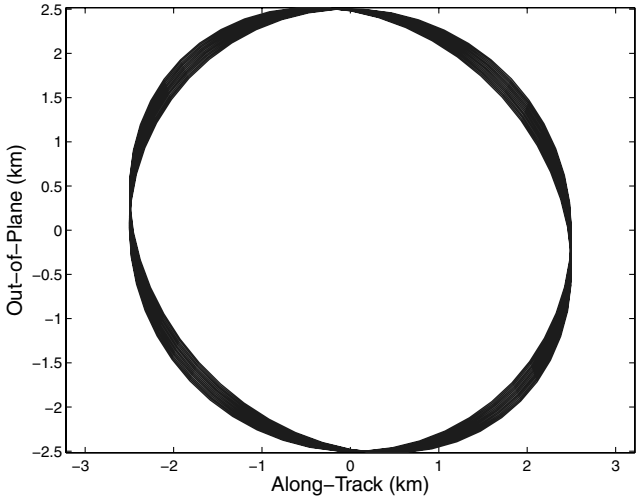

Fig. 2 Relative orbits for $i_0 = 90$ deg.

Amplitude Considerations

Attention in the preceding section was focused on the derivation of a frequency-matching condition in terms of i_0 and $\alpha(0)$. It is equally important to study the effect of these parameters on the cross-track amplitude growth-rate. In-plane amplitude variation is negligible, as long as Eq. (31) is satisfied.

Equation (19) can be expressed directly in terms of i_0 and $\alpha(0)$ via Eqs. (29), (30), and (34). The result obtained is

$$\rho_z \approx \rho\sqrt{1 + k^2 t^2 \sin^4 i_0 \cos^2\alpha(0) + kt\sin^2 i_0 \sin 2\alpha(0)} \tag{40}$$

Equation (40) shows that for nonequatorial orbits, cross-track amplitude growth rate is zero for the special case: $\alpha(0) = 90, 270$ deg or equivalently, for $\Delta i = 0$. Another special case of zero linear growth is obtained, corresponding to $\alpha(0) = 0$, 180 deg, by neglecting the t^2 term in Eq. (40). This assumption is reasonable for a time period of one day. Taken together, Eqs. (37–40) explain the existence of the so-called magic inclinations[¶] or frozen relative orbits.[**]

Relative orbits for other values of i_0, set up with the corresponding values of $\alpha(0)$, given by Eq. (37), are shown in Fig. 3 for a period of one day. The orbits in these figures do not precess, but show

[¶]Data available at http://www.esa.int/gsp/ACT/newsroom/NewsArchive/New17_Sep14_MagicInclinations.htm

[**]Suggested by Ronald J. Proulx, Charles Stark Draper Laboratory, Inc.

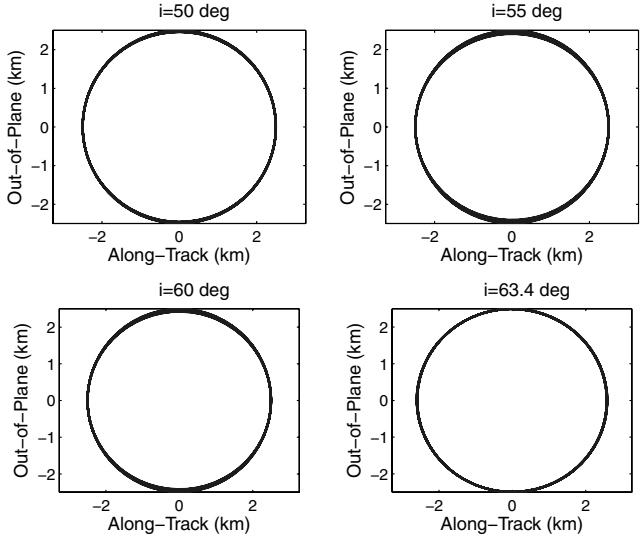

Fig. 3 Nonprecessing relative orbits for various inclinations (15 orbits shown for each inclination).

localized, cross-track growth for inclinations corresponding to $\alpha(0) \neq 0, 90$ deg. Note that the inclination chosen for the bottom-right figure (of Fig. 3) is not exactly the critical value, due to a singularity present in the mean-to-osculating element transformation [38].

Control Strategy and Thrust Acceleration Estimates Based on Modified HCW Equations

It is assumed in this section that the PCO initial conditions have been set up using Eqs. (26–31). The linearized relative motion of a deputy, when the chief is moving in a circular orbit, can be described by the HCW equations:

$$\ddot{x} - 2n_0\dot{y} - 3n_0^2 x = u_{x_{J2}} + u_{x_c} \tag{41}$$

$$\ddot{y} + 2n_0\dot{x} = u_{y_{J2}} + u_{y_c} \tag{42}$$

$$\ddot{z} + n_0^2 z = u_{z_{J2}} + u_{z_c} \tag{43}$$

where n_0 is the unperturbed two-body mean motion of the chief. The acceleration components in the right-hand side of the preceding equations can be separated into two parts: one due to J_2 and the other due to the action of thrust. The J_2-induced acceleration for PCO initial conditions can be estimated by substituting the perturbed motion variable expressions from Eqs. (11–13) in Eqs. (41–43). The deputy satellite's secular drift rates of mean anomaly and perigee are approximated by the respective drift rates of the chief. This approximation is consistent with the $\mathcal{O}(J_2)$ approximation of the disturbing accelerations. The results for the J_2-induced acceleration components are

$$u_{x_{J2}} = 3(\dot{M}_0^2 - n_0^2)x + 2(\dot{M}_0 - n_0)\dot{y} - 3n_0^2\Delta a \tag{44}$$

$$u_{y_{J2}} = -2(\dot{M}_0 - n_0)\dot{x} \tag{45}$$

$$u_{z_{J2}} = (n_0^2 - \dot{M}_0^2 - 2n_0\dot{\omega}_0)z - 2\rho(0)kn_0\sin^2 i_0 \cos\alpha(0)\sin\lambda_0 \tag{46}$$

A set of modified HCW equations are obtained by substituting Eqs. (44–46) into Eqs. (41–43):

$$\ddot{x} - 2\dot{M}_0\dot{y} - 3\dot{M}_0^2 x = u_{x_c} - 3n_0^2\Delta a \tag{47}$$

$$\ddot{y} + 2\dot{M}_0\dot{x} = u_{y_c} \tag{48}$$

$$\ddot{z} + \dot{M}_0^2 z = 2n_0\dot{\omega}_0 z - 2\rho(0)kn_0\sin^2 i_0 \cos\alpha(0)\sin\lambda_0 + u_{z_c} \tag{49}$$

It has been shown in [12,13] that a small, control-induced phase rotation rate $\dot{\alpha}$ is required for intersatellite fuel balancing. Hence, the reference motion variables are selected as

$$x(t) = 0.5\rho(0)\sin[\lambda_0(0) + \alpha(0) + (\dot{M}_0 + \dot{\alpha})t] + \Delta a \tag{50}$$

$$y(t) = \rho(0)\cos[\lambda_0(0) + \alpha(0) + (\dot{M}_0 + \dot{\alpha})t] \tag{51}$$

$$z(t) = \rho(0)\sin[\lambda_0(0) + \alpha(0) + (\dot{M}_0 + \dot{\alpha})t] \tag{52}$$

Note that the forms of Eqs. (51) and (52) do not match their respective initial values given by Eqs. (24) and (25), but the differences are negligible. It should also be noted that the reference motion representation chosen in this paper differs from those given in [12,13], because the perigee drift rate is not included in Eqs. (50–52). Furthermore, the differences between the natural motion variables, as given by Eqs. (14), (15), and (18) and those given by Eqs. (50–52), show that the chosen reference motion is not the natural motion, exactly. Hence, there is a need for feedback control in addition to the feedforward.

The following results for the control accelerations are obtained by substituting the previous reference variables into Eqs. (47–49):

$$u_{x_c} \approx \rho(0)n_0\dot{\alpha}\sin[\lambda_0(0) + \alpha(0) + (\dot{M}_0 + \dot{\alpha})t] \tag{53}$$

$$u_{y_c} \approx -\rho(0)n_0\dot{\alpha}\cos[\lambda_0(0) + \alpha(0) + (\dot{M}_0 + \dot{\alpha})t] \tag{54}$$

$$u_{z_c} \approx 2n_0(\dot{\omega}_0 - \dot{\alpha})\rho(0)\sin[\lambda_0(0) + \alpha(0) + (\dot{M}_0 + \dot{\alpha})t] + 2\rho(0)kn_0\sin^2 i_0 \cos[\alpha(0)]\sin\lambda_0 \tag{55}$$

Equations (53) and (54) indicate that the magnitudes of the in-plane thrust acceleration components for formation rotation depend linearly on $\dot{\alpha}$. Further insight on the dependence of the cross-track control acceleration magnitude on $\dot{\alpha}$ is obtained by squaring Eq. (55) and averaging the result over an orbit of the chief to eliminate the short-periodic variations. The mean square cross-track control acceleration is given as

$$u_{z_c}^2 = 2\rho^2(0)n_0^2\{(\dot{\omega}_0 - \dot{\alpha} + k\sin^2 i_0)^2\cos^2[\alpha(0)] + (\dot{\omega}_0 - \dot{\alpha})^2\sin^2\alpha(0)\} \tag{56}$$

The minimum value of $u_{z_c}^2$ is obtained for

$$\dot{\alpha} = \dot{\omega}_0 + k\sin^2 i_0\cos^2\alpha_0 = \dot{\omega}_0 + \dot{\psi} \tag{57}$$

This is not a surprising result, considering Eq. (38), which provides the expression for the natural cross-track phase angle rotation rate. For an orbit with inclination as given by Eq. (37), the optimal control-induced phase rotation rate is zero, because $\dot{\omega}_0 = -\dot{\psi}$. Thus, there is no need for the application of control for such a satellite, at least over a period of one day.

Formation Maintenance Without Radial Thrust

Before proceeding to model validation and simulation results, an important special case of control without the use of radial thrust is examined. It can be shown by using the in-plane motion variables and the modified HCW equations given by Eqs. (47) and (48) that, in addition to the savings resulting from not using radial thrust, there is also a reduction in the along-track control acceleration by 50%.

Successive differentiations of the in-plane equations and imposition of the zero-radial thrust constraint result in the following differential equation:

$$\dddot{y} + \dot{M}_0^2\ddot{y} = \ddot{u}_{y_c} - 3\dot{M}_0^2 u_{y_c} \tag{58}$$

In the absence of radial thrust, $x(t)$ does not follow the reference solution of Eq. (50), exactly. Substitution of Eq. (51) into Eq. (58) results in the following:

$$u_{x_c} = 0 \tag{59}$$

$$u_{y_c} = -0.5 n_0 \rho(0) \dot{\alpha} \cos[\lambda_0(0) + \alpha(0) + (\dot{M}_0 + \dot{\alpha})t] \tag{60}$$

$$x(t) = 0.5\left(1 + \frac{0.5\dot{\alpha}}{n_0}\right)\rho(0)\sin[\lambda_0(0) + \alpha(0) + (\dot{M}_0 + \dot{\alpha})t] + x_{\text{bias}} \tag{61}$$

where x_{bias} is a constant, to be defined later. A comparison of Eqs. (59) and (60) with Eqs. (53) and (54) shows the level of reduction in the net in-plane thrust acceleration achieved by not using radial thrust and relaxing the tracking requirement for the radial component of motion. The difference between the expressions in Eqs. (50) and (61) is $\mathcal{O}(J_2)$.

Radial Bias Component

The previous developments made use of the mean elements extensively. One can define and compute mean motion variables by using the differential mean elements instead of the differential osculating elements. However, because the averages of the short-periodic terms do not necessarily equal to zero, errors of $\mathcal{O}(J_2)$ can result in some of the relative motion variables due to a direct substitution of the mean elements. Sengupta et al. [34] have obtained corrections to the mean motion variables, resulting in the so-called averaged expressions for the relative motion variables. This analytical filtering process removes the short-periodic oscillations from a function f of the osculating element vector $\mathcal{Æ}$ via the following transformation:

$$f_{\text{av}}(\mathcal{Æ}) = f(\bar{\mathcal{Æ}}) + \frac{1}{2\pi}\int_0^{2\pi} f_{\text{sp}}(\bar{\mathcal{Æ}})\,\mathrm{d}M \tag{62}$$

where f_{av} is the average of f, $\bar{\mathcal{Æ}}$ indicates the mean element vector, and f_{sp} denotes the short-periodic variations of f. Details of obtaining the required f_{sp} expressions and the results for the filtered relative motion variables for eccentric orbits are presented in detail in [34]. Of significance to the present work is the correction to the radial bias expression obtained in [34] for circular orbits:

$$x_{\text{bias}} \approx \Delta a + \frac{9}{4}J_2\left(\frac{R_e}{a_0}\right)^2 a_0 \sin(2i_0)\Delta i \tag{63}$$

Substitutions of the expression for Δa given by Eq. (31) and that for Δi from Eq. (30) into the preceding equation, result in

$$x_{\text{bias}} \approx -\frac{5}{4}J_2\rho(0)\left(\frac{R_e}{a_0}\right)^2 \sin(2i_0)\cos\alpha(0) \tag{64}$$

The expression for x_{bias} can be substituted in Eq. (61); it is essential for achieving additional fuel savings.

Fuel Minimization and Balancing

Balancing the rate of fuel consumption among identical satellites in a formation results in a common ballistic coefficient for all the satellites. This is important, because differential drag has not been accounted for. Assuming that radial thrust is not used, the mean square control acceleration, averaged over an orbit, can be evaluated as shown next:

$$J = \frac{n_0}{2\pi}\int_0^{2\pi/n_0} (u_{y_c}^2 + u_{z_c}^2)\,\mathrm{d}t \tag{65}$$

The performance index defined here is amenable to a simple analysis but, in general, it does not accurately represent the fuel requirement. However, J is directly proportional to the fuel consumption for power-limited, low-thrust propulsion.

The following expression for J is obtained by substituting Eqs. (55) and (60) into Eq. (65) and evaluating the integral:

$$J = (\rho n_0)^2\left[\frac{1}{8}\dot{\alpha}^2 + 2(\dot{\alpha} - \dot{\omega}_0)^2 + 2k^2\sin^4 i_0\cos^2\alpha_0 - 4(\dot{\alpha} - \dot{\omega}_0)k\sin^2 i_0\cos^2\alpha_0\right] \tag{66}$$

The averaged cost per satellite, considering an infinite number of satellites, over one orbit of the chief, can be represented as

$$J_{\text{formation}} = \frac{n_0}{4\pi^2}\int_0^{2\pi/n_0}\int_0^{2\pi} (u_{y_c}^2 + u_{z_c}^2)\,\mathrm{d}\alpha(0)\,\mathrm{d}t \tag{67}$$

Evaluation of the preceding integral results in the following:

$$J_{\text{formation}} = (\rho n_0)^2\left[\frac{1}{8}\dot{\alpha}^2 + 2(\dot{\alpha} - \dot{\omega}_0)^2 + k^2\sin^4 i_0 - 2(\dot{\alpha} - \dot{\omega}_0)k\sin^2 i_0\right] \tag{68}$$

Minimization of the preceding expression with respect to $\dot{\alpha}$ yields

$$\dot{\alpha}_{\text{opt}_{\text{formation}}} = \frac{16}{17}\left(\dot{\omega}_0 + \frac{1}{2}k\sin^2 i_0\right) = \frac{16}{17}(\dot{\omega}_0 + \dot{\psi}_{\text{av}}) \tag{69}$$

For each deputy in the formation, the optimal phase rotation rate, as a function of its initial phase angle, is given by

$$\dot{\alpha}_{\text{opt}_{\text{satellite}}} = \frac{16}{17}(\dot{\omega}_0 + k\sin^2 i_0\cos^2\alpha_0) = \frac{16}{17}(\dot{\omega}_0 + \dot{\psi}) \tag{70}$$

Equations (57) and (70) are closely related. Whereas the result of Eq. (57) is obtained by minimizing the out-of-plane thrust acceleration only, the result of Eq. (70) minimizes the total cost. Hence, the optimal value of $\dot{\alpha}$ is dictated predominantly by the out-of-plane dynamics. These results are valid only for the quadratic performance index in Eq. (65). The optimal rate of phase shift for a formation is independent of the radius of the relative orbit and is $\mathcal{O}(J_2 n_0)$.

Figure 4 shows the variation of $\dot{\alpha}$ for a formation, as well as two individual satellites, one with $\alpha(0) = 0$ and the other with $\alpha(0) = 90$ deg. There exist multiple i_0 and $\alpha(0)$ pairs satisfying Eq. (37) for which $\dot{\alpha} = 0$ is optimal. For a formation, the required $\dot{\alpha}$ is zero if i_0 is equal to 54.73 deg or its supplement, the values for which the perturbed mean motion is equal to the two-body mean motion. For such a formation, $\dot{\omega}_0$ is equal and opposite of $\dot{\psi}_{\text{av}}$.

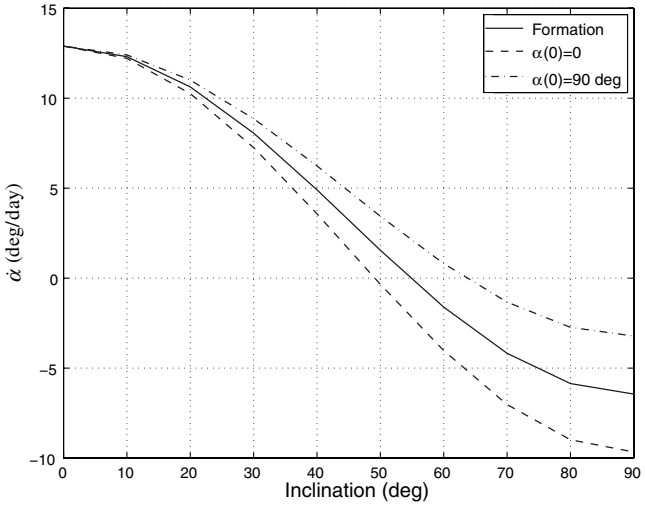

Fig. 4 Optimal phase rotation rate as a function of inclination.

The costs for individual satellites, as well as the average formation-maintenance cost can also be minimized with respect to inclination. Simultaneous minimization of J, given by Eq. (66) with respect to i_0 and $\alpha(0)$, results in the following:

$$i_0^{**} = \sin^{-1}\left(\sqrt{\frac{20 + 8\cos^2\alpha(0)}{88\cos^2\alpha(0) - 64\cos^4\alpha(0) + 25}}\right) \tag{71}$$

As can be seen from Eq. (71), for a satellite with $\alpha(0) = 0$, $i_0^{**} = i_0^* = 49.11$ deg. Similarly, the critical inclination value is optimal for a satellite with $\alpha(0) = 90$ deg. The value of i_0^{**} for a formation can be obtained from Eqs. (68) and (69) or, directly, by substituting in Eq. (71), $\cos^2\alpha(0) = 0.5$. The result is $i_0^{**} = 42.3$ deg.

Control acceleration for formation keeping, with respect to the reference trajectory chosen, is required to mitigate two effects: 1) frequency mismatch and 2) cross-track amplitude variation. The i_0–$\alpha(0)$ constraint given by Eq. (37) automatically accounts for the first effect, but not the second. Equations (37) and (71) are simultaneously satisfied for $i_0 = 49.11$ deg and the critical inclination.

Linear Quadratic Regulator Control Using Averaging Filter

The steady-state, continuous-time, LQR control method based on the standard HCW model is used for formation maintenance, resulting in a constant-gain, tracking control law. In this work, the feedback controls are augmented with the feedforward controls given by Eqs. (55) and (60):

$$\begin{bmatrix} u_y \\ u_z \end{bmatrix} = \begin{bmatrix} u_{y_c} \\ u_{z_c} \end{bmatrix} - \mathbf{K}\begin{bmatrix} \mathbf{x} - \mathbf{x}_r \\ \dot{\mathbf{x}} - \dot{\mathbf{x}}_r \end{bmatrix} \tag{72}$$

where $\mathbf{K}$ is the LQR gain matrix and $\mathbf{x} = [x \quad y \quad z]^\top$. The reference position vector $\mathbf{x}_r$ is obtained from Eqs. (51), (52), and (61).

Beginning with a set of mean classical elements for the chief, the initial mean elements can be setup for a deputy satellite with the selection of ρ and $\alpha(0)$ via Eqs. (26–31) for the differential mean classical elements. It is best to use the method of Gim and Alfriend [39] for the mean-to-osculating transformation for near-circular orbits. This procedure has been developed for nonsingular as well as equinoctial elements. The osculating orbital elements can be converted into inertial position and velocity vectors to obtain the initial conditions for a numerical integration process. The relative position and velocity states are obtained from the inertial states of the satellites by using the transformations presented in [40]. Next, the relative state is filtered [34] to remove the short-periodic oscillations and then feedback via the control law given by Eq. (72).

Simulation Results

Simulations were carried out by using the inertial coordinate representations of the nonlinear equations of motion of the individual satellites. A formation of seven satellites was set up in a 1 km, PCO configuration with initial phase angles ranging from 0 to 90 deg. The chief was assumed to be in a circular orbit with mean $a = 7100$ km and 1500 orbits (equivalent to $\approx$100 days) were propagated. The control weights were chosen to be diagonal: $[1, 1]/n_0^4$, the state weight matrix was selected with unit weights for the position coordinates, and the rate error weight for each axis was n_0^{-2}.

Figure 5 shows the individual satellite cost functions for $i_0 = 49.11$ deg, obtained by evaluating Eq. (65) for each deputy and extrapolating the value over a period of 1 year. The variations of the cost are shown for two cases, with and without fuel balancing. Each line in this figure represents a single satellite. The fuel-balanced cost curves are close to each other and have a smaller average slope compared with the unbalanced cost curves. Hence, the average rate of fuel consumption with $\dot{\alpha} = 0$ is higher than that with $\dot{\alpha}_{\text{opt}} = 1.84$ deg/day, the corresponding optimal rate. As can be seen from the figure, the use of the optimal rotation rate reduces the

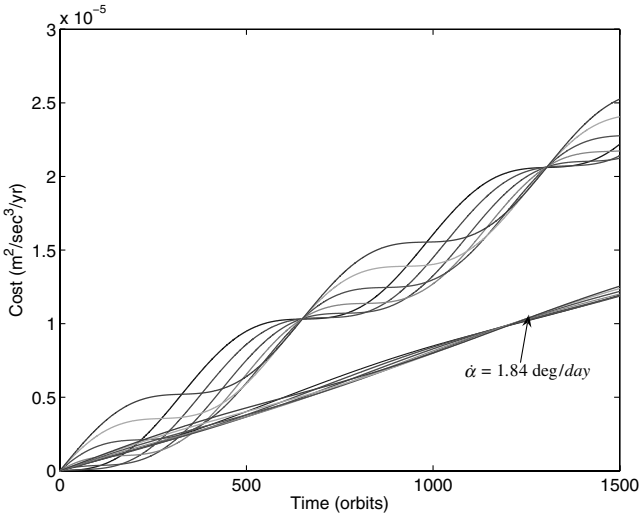

Fig. 5 Cost vs time with and without $\dot{\alpha}$, $i_0 = 49.11$ deg, 1500 orbits.

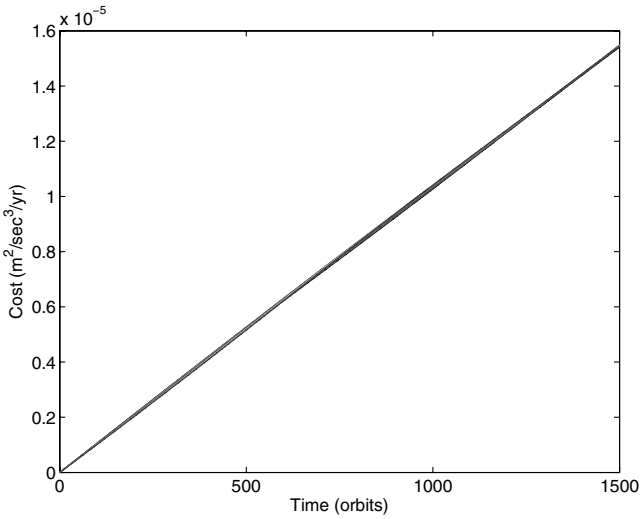

Fig. 6 Cost vs time with $\dot{\alpha} = 0$, $i_0 = 54.73$ deg, 1500 orbits.

formation-maintenance cost and simultaneously balances the intersatellite fuel requirements to a great extent. The fuel curves for $\dot{\alpha} = 0$ do coincide periodically, but their short-term variations are appreciable. The total formation-maintenance cost with fuel balancing, evaluated from the simulation results, is 8.49×10^{-5} m^2/s^3/year compared to a cost of 1.59×10^{-4} m^2/s^3/year, obtained by holding α constant for each satellite.

Figure 6 shows that natural fuel balancing takes place for a formation with $i_0 = 54.73$ deg without a control-induced formation rotation. The total formation-maintenance cost for this case is 1.08×10^{-4} m^2/s^3/year. This value of the inclination is ideal for fuel balancing, but not for the best fuel economy, because the average rate of fuel consumption is higher for this case as compared with that for $i_0 = 49.11$ deg.

As shown in Fig. 7, the formation-maintenance cost for $i_0 = 42.3$ deg is 7.58×10^{-5} m^2/s^3/year, slightly better than that for $i_0 = 49.11$ deg. Figure 8 shows a cost comparison with and without fuel balancing for $i_0 = 70$ deg. The fuel-balanced cost curves are very close to each other and can be easily distinguished from their counterparts. The optimal rotation rate for this case is $\dot{\alpha}_{\text{opt}} = -4.1827$ deg/day. The total cost with fuel balancing is 2.12×10^{-4} m^2/s^3/year compared with 5.56×10^{-4} m^2/s^3/year, without.

The preceding results also point out that longer-term extrapolations of fuel requirements for individual satellites, based on short-term simulations, can be erroneous, especially when the individual costs are not well balanced. However, it is reasonable to

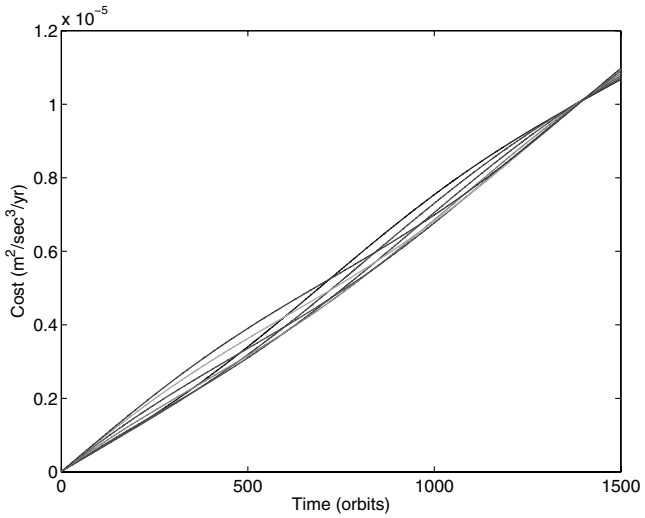

Fig. 7 Cost vs time with $\dot{\alpha} = 4.13\,\text{deg/day}$, $i_0 = 42.3\,\text{deg}$, 1500 orbits.

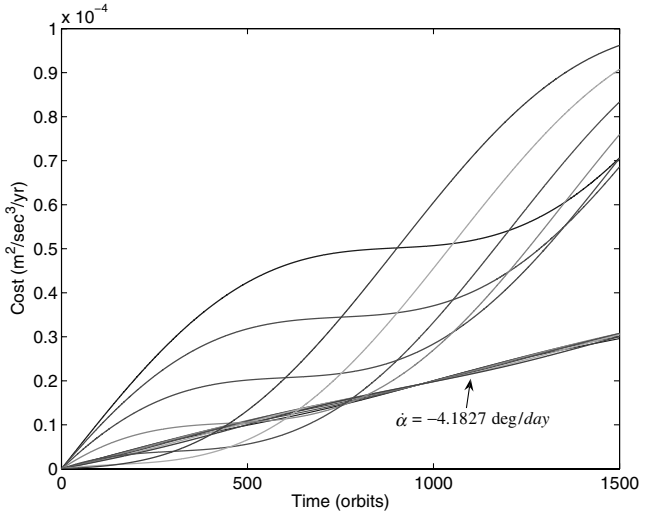

Fig. 8 Cost vs time with and without $\dot{\alpha}$, $i_0 = 70\,\text{deg}$, 1500 orbits.

extrapolate the total fuel consumption for a formation, over extended periods of time, because the process of cost averaging virtually eliminates the periodic effects. As can be seen from Figs. 5–8, cost curves for the individual satellites show significant periodic behavior, superimposed over the mean variation, for $\dot{\alpha} = 0$. The periodic components of the cost curves are negligible compared with their respective linear-growth terms when the fuel consumption is well balanced.

Figures 9 and 10 show the plots of the along-track and cross-track components of the total and feedforward controls for a deputy with $\alpha(0) = 0$ and for $i_0 = 70\,\text{deg}$ over 15 orbits. The fundamental frequencies of the feedback and feedforward controls for each axis are equal to each other. There is a long-period variation in the cross-track control, appearing as a secular component in Fig. 10. Twice-per-orbit components in the total controls are also present for both the axes, as can be ascertained from Fig. 11, which shows the differences between the two acceleration components for each axis. A small bias component is also visible in the cross-track acceleration error. These effects are caused by the differential eccentricity of the orbit of the deputy, a higher-order effect neglected in the preceding analysis.

Conclusions

This paper has developed expressions for the fundamental frequencies of J_2-perturbed relative motion of satellites in near-circular orbits. Special inclination-phase-angle combinations have been obtained, for which the in-plane and out-of-plane fundamental

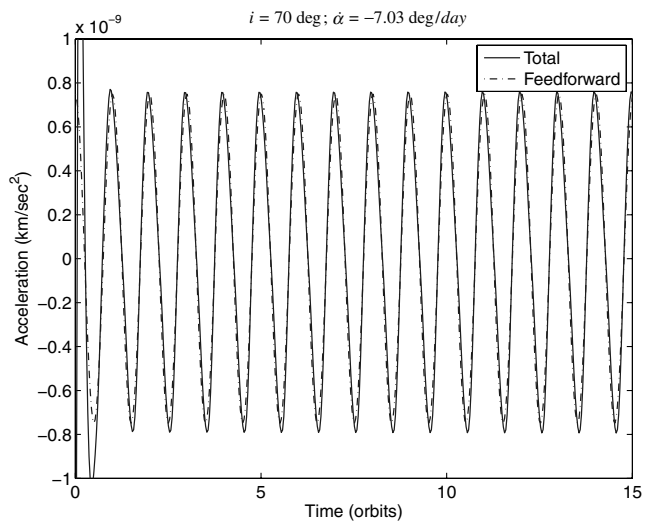

Fig. 9 Comparison of total and feedforward along-track controls.

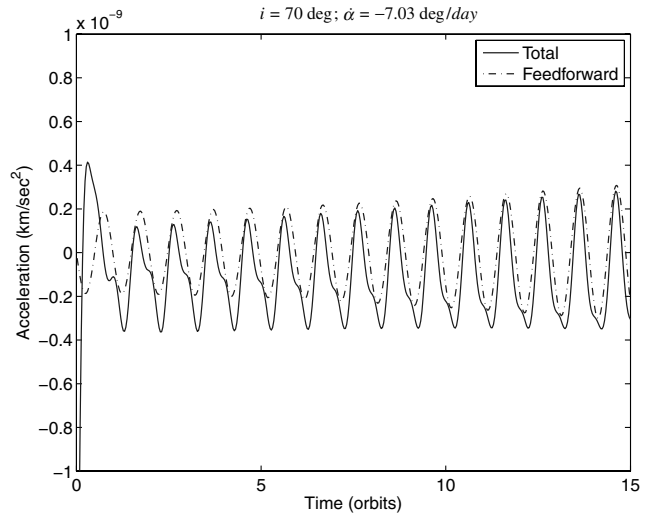

Fig. 10 Comparison of total and feedforward cross-track controls.

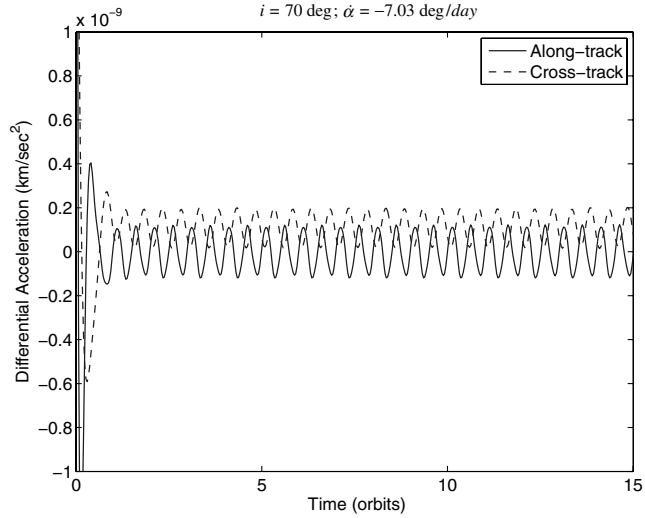

Fig. 11 Differences between total and feedforward accelerations.

frequencies are equal, over an extended period of time. The resulting relative orbits do not precess and, under further restrictions, do not distort in the presence of differential nodal precession. These results validate and generalize previously reported numerical findings in [32]. Special values of the orbit inclination have been identified for minimizing control requirements for individual satellites as well as for a formation. Accurate estimates of the control requirements for formation maintenance and intersatellite fuel balancing have also been presented. The advantage of not using the radial component of thrust has been clearly demonstrated, especially for circular reference orbits. Higher-order terms can be retained in the approximations, as well as the reference trajectories, to improve the results of this paper.

Acknowledgment

This research was funded in part by support from the U.S. Air Force Research Laboratory through the Consortium for Autonomous Space Systems project at Texas A&M University.

References

[1] Scharf, D. A., Hadaegh, F. Y., and Ploen, S. R., "Survey of Spacecraft Formation Flying Guidance and Control, Part 1: Guidance," *Proceedings of the American Control Conference*, Vol. 2, American Automatic Control Council, Evanston, IL, June 2003, pp. 1733–1739.

[2] Kong, E., Kwon, D., Schweighart, S., Elias, L., Sedwick, R., and Miller, D., "Electromagnetic Formation Flight for Multi-Satellite Arrays," *Journal of Spacecraft and Rockets*, Vol. 41, No. 4, July–Aug. 2004, pp. 659–666.
doi:10.2514/1.2172

[3] King, L. B., Parker, G. G., Deshmukh, S., and Chong, J.-H., "Study of Interspacecraft Coulomb Forces and Implications for Formation Flying," *Journal of Propulsion and Power*, Vol. 19, No. 3, May–June 2003, pp. 497–505.

[4] Clohessy, W. H., and Wiltshire, R. S., "Terminal Guidance System for Satellite Rendezvous," *Journal of the Astronautical Sciences*, Vol. 27, No. 9, Sept. 1960, pp. 653–678.

[5] Alfriend, K. T., Schaub, H., and Gim, D.-W., "Gravitational Perturbations, Nonlinearity and Circular Orbit Assumption Effects on Formation Flying Control Strategies," *Advances in the Astronautical Sciences*, Vol. 104, No. 104, 2000, pp. 139–158.

[6] Garrison, J. L., Gardner, T. J., and Axelrad, P., "Relative Motion in Highly Elliptical Orbits," *Advances in the Astronautical Sciences*, Vol. 89, No. 2, 1995, pp. 1359–1376.

[7] Inalhan, G., Tillerson, M. J., and How, J., "Relative Dynamics and Control of Spacecraft Formations in Eccentric Orbits," *Journal of Guidance, Control, and Dynamics*, Vol. 25, No. 1, 2002, pp. 48–59.

[8] Lane, C. M., and Axelrad, P., "Formation Design in Eccentric Orbits Using Linearized Equations of Relative Motion," *Journal of Guidance, Control, and Dynamics*, Vol. 29, No. 1, 2006, pp. 146–160.
doi:10.2514/1.13173

[9] Schaub, H., "Spacecraft Relative Orbit Description through Orbit Element Differences," *14th U. S. National Congress of Theoretical and Applied Mechanics*, 2002.

[10] Schaub, H., "Relative Orbit Geometry Through Classical Orbit Element Differences," *Journal of Guidance, Control, and Dynamics*, Vol. 27, No. 5, 2004, pp. 839–848.
doi:10.2514/1.12595

[11] Sengupta, P., and Vadali, S. R., "Relative Motion and the Geometry of Formations in Keplerian Elliptic Orbits," *Journal of Guidance, Control, and Dynamics*, Vol. 30, No. 4, 2007, pp. 953–964.
doi:10.2514/1.25941

[12] Vadali, S. R., Vaddi, S. S., and Alfriend, K. T., "Intelligent Control Concept for Formation Flying Satellite Constellations," *International Journal of Robust and Nonlinear Control*, Vol. 12, Nos. 2–3, 2002, pp. 97–115.
doi:10.1002/rnc.678

[13] Vadali, S. R., Vaddi, S. S., Naik, K., and Alfriend, K. T., "Control of Satellite Formations," *Proceedings of the AIAA Guidance Navigation and Control Conference*, AIAA Paper 2001-4028, Aug. 2001.

[14] Zanon, D. J., and Campbell, M. E., "Optimal Planner for Spacecraft Formations in Elliptical Orbits," *Journal of Guidance, Control, and Dynamics*, Vol. 29, No. 1, 2006, pp. 161–171.
doi:10.2514/1.7236

[15] Gurfil, P., "Relative Motion Between Elliptic Orbits: Generalized Boundedness Conditions and Optimal Formationkeeping," *Journal of Guidance, Control, and Dynamics*, Vol. 28, No. 4, July–Aug. 2005, pp. 761–767.
doi:10.2514/1.9439

[16] Kasdin, N. J., and Kolemen, E., "Bounded, Periodic Relative Motion Using Canonical Epicyclic Orbital Elements," *Advances in the Astronautical Sciences*, Vol. 120, No. 2, Jan. 2005, pp. 1381–1398; also American Astronautical Society Paper 05-186, 2005.

[17] Kolemen, E., and Kasdin, N. J., "Relative Spacecraft Motion: A Hamiltonian Approach to Eccentricity Perturbations," *Advances in the Astronautical Sciences*, Vol. 119, No. 3, Feb. 2004, pp. 3075–3086; also American Astronautical Society Paper 04-294, 2004.

[18] Sengupta, P., Sharma, R., and Vadali, S. R., "Periodic Relative Motion near a Keplerian Elliptic Orbit with Nonlinear Differential Gravity," *Journal of Guidance, Control, and Dynamics*, Vol. 29, No. 5, 2006, pp. 1110–1121.
doi:10.2514/1.18344

[19] Vaddi, S. S., Vadali, S. R., and Alfriend, K. T., "Formation Flying: Accommodating Nonlinearity and Eccentricity Perturbations," *Journal of Guidance, Control, and Dynamics*, Vol. 26, No. 2, 2003, pp. 214–223.

[20] de Queiroz, M. S., Kapila, V., and Yan, Q., "Adaptive Nonlinear Control of Multiple Spacecraft Formation Flying," *Journal of Guidance, Control, and Dynamics*, Vol. 23, No. 3, May–June 2000, pp. 385–390.

[21] Schaub, H., and Alfriend, K. T., "Impulse Feedback Control to Establish Specific Mean Orbit Elements of Spacecraft Formations," *Journal of Guidance, Control, and Dynamics*, Vol. 24, No. 4, July–Aug. 2001, pp. 739–745.

[22] Schaub, H., and Alfriend, K. T., "Hybrid Cartesian and Orbit Element Feedback Law for Formation Flying Spacecraft," *Journal of Guidance, Control, and Dynamics*, Vol. 25, No. 2, March–April 2002, pp. 387–393.

[23] Schaub, H., Vadali, S. R., Junkins, J. L., and Alfriend, K. T., "Spacecraft Formation Flying Using Mean Orbital Elements," *Journal of the Astronautical Sciences*, Vol. 48, No. 1, Jan.–March 2000, pp. 69–87.

[24] Ulybyshev, Y., "Long-Term Formation Keeping of Satellite Constellation Using Linear Quadratic Controller," *Journal of Guidance, Control, and Dynamics*, Vol. 21, No. 1, Jan.–Feb. 1998, pp. 109–115.

[25] Vaddi, S. S., Alfriend, K. T., Vadali, S. R., and Sengupta, P., "Optimal Formation Establishment and Reconfiguration Using Impulsive Control," *Journal of Guidance, Control, and Dynamics*, Vol. 28, No. 2, March–April 2005, pp. 262–268.
doi:10.2514/1.6687

[26] Vaddi, S. S., and Vadali, S. R., "Linear and Nonlinear Control Laws for Formation Flying," *Proceedings of the AAS/AIAA Space Flight Mechanics Conference*, Vol. 114, Univelt, San Diego, CA, Feb. 2003.

[27] Izzo, D., Sabatini, M., and Valente, C., "New Linear Model Describing Formation Flying Dynamics Under J2 Effects," *Proceedings of the 17th AIDAA National Congress*, Vol. 1, Italian Association of Aeronautics and Astronautics, Milan, 2003, pp. 493–500.

[28] Schweighart, S. A., and Sedwick, R. J., "High-Fidelity Linearized J2 Model for Satellite Formation Flight," *Journal of Guidance, Control, and Dynamics*, Vol. 25, No. 6, Nov.–Dec. 2002, pp. 1073–1080.

[29] Vadali, S. R., Alfriend, K. T., and Vaddi, S. S., "Hill's Equations, Mean Orbital Elements, and Formation Flying of Satellites," *Advances in the Astronautical Sciences*, Vol. 106, March 2000, pp. 187–204; also American Astronautical Society Paper 00-258, 2000.

[30] McLaughlin, C. A., Sabol, C., Swank, A., Burns, R., and Luu, K., "Modeling Relative Position, Relative Velocity, and Range Rate for Formation Flying," *Advances in the Astronautical Sciences*, Vol. 109, No. 3, 2001, pp. 2165–2186; also American Astronautical Society Paper 01-457, 2001.

[31] Sabol, C., Burns, R., and McLaughlin, C. A., "Satellite Formation Flying Design and Evolution," *Journal of Spacecraft and Rockets*, Vol. 38, No. 2, March–April 2001, pp. 270–278.

[32] Sabatini, M., Izzo, D., and Bevilacqua, R., "Special Inclinations Allowing Minimal Drift Orbits for Formation Flying Satellites," *Journal of Guidance, Control, and Dynamics*, Vol. 31, No. 1, Jan.–Feb. 2008, pp. 94–100.
doi:10.2514/1.30314

[33] Vadali, S. R., "Analytical Solution for Relative Motion of Satellites," *Dynamics and Control of Systems and Structures in Space 2002*, Cranfield Univ., Cranfield, UK, July 2002, pp. 309–316.

[34] Sengupta, P., Vadali, S. R., and Alfriend, K. T., "Averaged Relative Motion and Applications to Formation Flight near Perturbed Orbits," *Journal of Guidance, Control, and Dynamics*, Vol. 31, No. 2, 2008, pp. 258–272.
doi:10.2514/1.30620

[35] Schaub, H., and Alfriend, K. T., "J2-Invariant Relative Orbits for Formation Flying," *Celestial Mechanics and Dynamical Astronomy*, Vol. 79, No. 2, Feb. 2001, pp. 77–95.
doi:10.1023/A:1011161811472

[36] Breger, L. S., "Control of Spacecraft in Proximity Orbits," Ph.D. Dissertation, Dept. of Aeronautics and Astronautics, Massachusetts Inst. of Technology, Cambridge, MA, June 2007.

[37] Yan, K., Alfriend, K. T., Vadali, S. R., and Sengupta, P., *Optimal Design of Satellite Formation Relative Motion Orbits Using Least Squares Methods*, Univelt, San Diego, CA, 2007, pp. 1467–1484; also American Astronautical Society Paper 07-199, 2007.

[38] Brouwer, D., "Solution of the Problem of Artificial Satellite Theory Without Drag," *Astronomical Journal*, Vol. 64, Nov. 1959, pp. 378–397.
doi:10.1086/107958

[39] Gim, D.-W., and Alfriend, K. T., "State Transition Matrix of Relative Motion for the Perturbed Noncircular Reference Orbit," *Journal of Guidance, Control, and Dynamics*, Vol. 26, No. 6, Nov.–Dec. 2003, pp. 956–971.

[40] Vadali, S. R., Schaub, H., and Alfriend, K. T., "Initial Conditions and Fuel-Optimal Control for Formation Flying of Satellites," *Proceedings of the AIAA GNC Conference*, AIAA Paper 99-4265, Aug. 1999.